# Computational Mechanics Analysis in Elevated Shell Platform Structures

*Azizah Abdul Nassir, Yee Hooi Min*, Syahrul Fithry Senin*
*Universiti Teknologi MARA, Cawangan Pulau Pinang,*
*13500 Permatang Pauh, Pulau Pinang, Malaysia.*
**minyh@uitm.edu.my*

ABSTRACT

*Shell structures are usually used in roof applications and aerospace structures. The advantage of these structures is not fully utilized in transmitting applied force. A thin-shell structure can be used for building construction and aerospace structures due to its lightweight nature. The township high load in this study refers to the high-speed airflow in the case of aerospace. This study was conducted to justify the feasibility of applying a thin-shell structure as an elevated shell platform for township foundations, where several different geometries were analyzed using finite element analysis (FEA) and artificial neural network (ANN). In the findings, all maximum stresses from different geometries are lower than the design value, thus verifying the feasibility of constructing a shell platform for heavy loading applications. The regression plots from the ANN output show that all geometries approached the value of 1, which means that the predicted ANN output and actual datasets of FEA are almost similar. From the ANN predicted output, the mean square error (MSE) was calculated. All the MSE values obtained from each geometry approached zero, indicating the analysis is precise and has a minimal error. Thus, this study has justified the feasibility of proposing elevated shells for township applications, which can be used as a reference in the design phase for future implementation.*

**Keywords:** *Shell structure; Township; Finite element analysis; Artificial neural network; Stresses; Deformation; Regression*

ISSN 1823-5514, eISSN 2550-164X

Received for review: 2021-01-22
Accepted for publication: 2021-05-20
Published: 2021-09-15

## Introduction

The construction of a shell roof structure is economical as it provides a large space area without any column underneath. The ability of the structure to resist its own load under normal stresses is economical in terms of material [1]. A thin-shell structure eliminates the requirement of higher thickness due to the lower bending moment to resist, which is categorized as a lightweight structure. In aerospace system design, the improvement in-flight performance, such as better acceleration, higher structural strength and stiffness, and better safety performance, can also be achieved by lightweight design [2]. A shell has an unstressed state compared to a flat plate due to its curvature [3].

Flood is the current arising issue in Malaysia that severely affects people, and most of them experienced damaged houses caused by the disaster. There is still no implementation of an elevated platform as an alternative in minimizing the damage caused by the catastrophic event. Cyclic loads from structural defects and failures in buildings are a real concern as natural disasters can cause serious damage to both offshore and onshore structures [4]. Thus, this study has proposed an elevated shell structure to minimize the damage caused by natural disasters.

Several investigations about shell structures have been made but limited to roof structures only. Some of the values and formulas are included in calculations and all the references have been cited in this paper. A study on stress and deflection of folded plates and cylindrical shells found that barrel roofs produced lower stresses and deflections than folded plates. This is due to different surface profiles affecting the load distribution for both shells [5]. A curve folded shell was investigated to study the effect of surface configuration with a fixed support condition. The finding showed that the highest deflection occurred at the center of the shell's surface [6]. Therefore, the proposed geometries in this study have different surface profiles to study the effect on load distribution and stresses while resisting the load of the township.

Research on strengthening an open support elliptical paraboloid concrete shell justified that the failure load increased to 14% for shells with non-continuous support compared to shells with continuous support [7]. Standard guidelines and historical data for flood have been used in this paper to identify the required minimum dimensions of the shell proposed. The minimum clear vertical height must be more than 6.5 m [8]. In Malaysia, it was found that the worst flood level was 2.11 m above the danger level [9].

## Methodology

Three different geometries were chosen to be analyzed: dome, cone, and toroidal. Constant dimensions and parameters were used to study the effect of different geometries in township implementation. A convergence test can be used to verify the approximation in the method applied [10]. Thus, the convergence test was performed to identify the height of the shell in this study. The value of the diameter calculated can fit up to 230 houses, which is the common total number of houses constructed for residential development. The boundary condition for all geometries is fixed support to simulate the actual conditions in construction. The dimensions of the shell proposed are shown in Table 1.

Table 1: Dimensions of proposed shell structure platform

| Parameters | Unit | Values |
|---|---|---|
| Height | m | 20 |
| Diameter | m | 200 |
| Thickness | m | 0.3 |
| Distributed Load | kN/m$^2$ | 20 |
| Material | - | Concrete |
| Density | kN/m$^3$ | 24 |
| Characteristic Strength, fck (Design value) | N/mm$^2$ | 40 |

The characteristic strength of concrete is one of the important parameters in this study, which is used to justify the feasibility of the proposed shell in resisting the heavy loading applied. In the design term, this characteristic strength is the ultimate compression strength where the material will fail or break when the maximum stress generated is exceeding the ultimate value. For this study, the concrete grade chosen is C40 with a 40 N/mm$^2$ design value that is commonly applied for foundation or substructure.

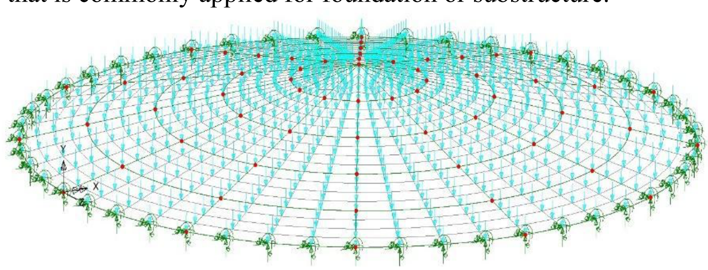

Figure 1: Structural modelling with loading and boundary conditions.

LUSAS software was utilized in modelling and analysis phases to study the stress, load distribution, and deformation of geometries. The outputs were extracted into an artificial neural network (ANN) computing system using

MATLAB software. The data extracted include node coordinates, note rotation, and node deformation. The ANN output produces a regression graph indicating the relationship between the input and output of the data. From the regression graph, the correlation coefficient, r should be near 1, which means that there is a positive relationship between the data [11]. Meanwhile, the mean squared error (MSE) can be calculated to justify that the neuron output matches the actual neuron output when the MSE calculated approaches 0 [12]. The visualization of the structures with the load applied and the boundary conditions are shown in Figure 1. The number of nodes and members for each geometric is listed in Table 2.

Table 2: Total number of nodes and members for each geometrics

| Geometric | Total number of nodes | Total number of element plane |
|---|---|---|
| Dome | 2752 | 900 |
| Toroidal | 1889 | 960 |
| Cone | 937 | 912 |

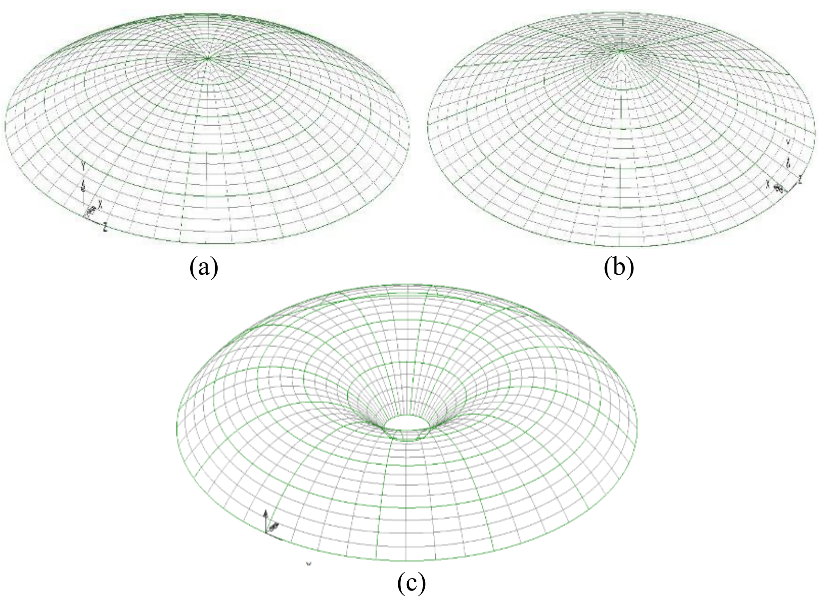

(a) (b) (c)

Figure 2: (a) Modelling of dome geometric, (b) Modelling of cone geometric, (c) Modelling of toroidal geometric.

## Results and Discussion

### Modelling of shell

Three different geometries proposed for this study are dome, cone, and toroidal. The modelling was done using LUSAS software, and the outputs are presented in Figure 2.

### Maximum stresses

The stress distribution contours for all geometries are shown in Table 3, Table 4, and Table 5. Based on the equivalent resultant stress contours of all geometries, the dome geometry distributed the load uniformly along its surface. Meanwhile, the toroidal geometry showed that the high stress concentrated at the middle of the boundary condition, and the rest of the surface recorded the lowest value of stress. On the other hand, the cone geometry showed that the high stress concentrated at the peak of the geometry. This is due to the different surface profiles of each geometry and its boundary conditions. The maximum stress was calculated using Equation (1) [13] and tabulated in Table 6.

$$Maximum\ stress = \frac{NE}{t} \quad (1)$$

where $N_E$ is the equivalent resultant stress and $t$ is the thickness of the shell structure. Equivalent stress is the combination of individual component stresses in direction X and direction Y, in a scalar stress state [14]. The values are obtained from software output based on the von Mises yield criterion [15]. For a shell structure, the resultant stress is expressed in force per unit length.

Thus, to obtain the maximum stress generated by each geometry, the resultant stress should be divided by the thickness to convert the stress into per unit area.

Table 3: Stresses contour of dome geometric

<table>
<tr><th>Stresses</th><th>Contour</th></tr>
<tr><td>Stress Resultant in Local X, Nx</td><td>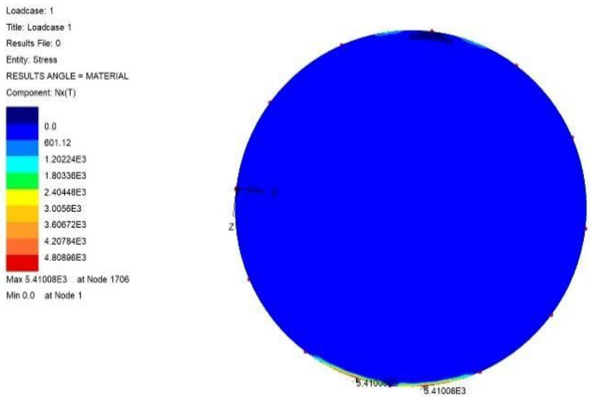
</td></tr>
<tr><td>Stress Resultant in Local Y, Ny</td><td>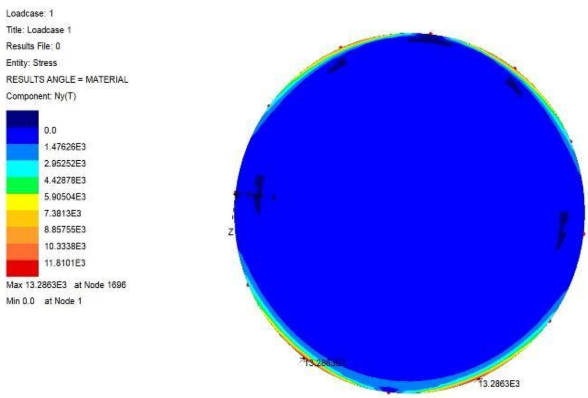
</td></tr>
<tr><td>Equivalent Resultant Stress, Ne</td><td>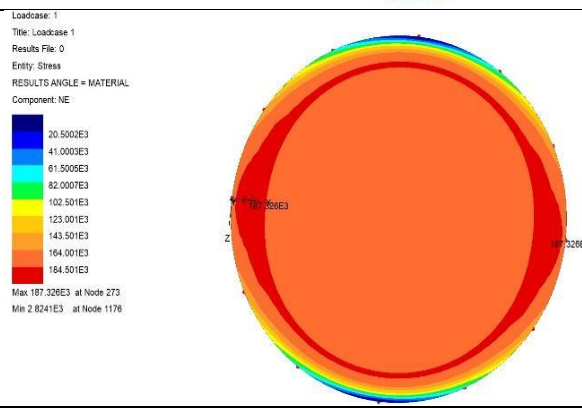
</td></tr>
</table>

Table 4: Stresses contour of toroidal geometric

| Stresses | Contour |
|---|---|
| Stress Resultant in Local X, Nx | 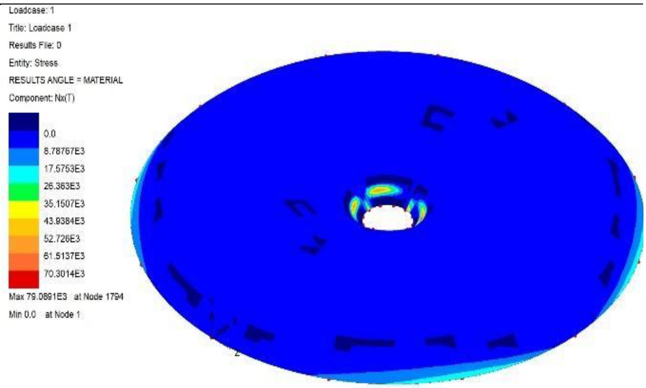 |
| Stress Resultant in Local Y, Ny | 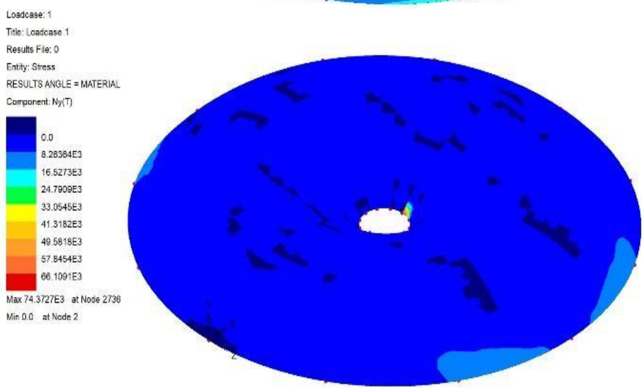 |
| Equivalent resultant stress, Ne | 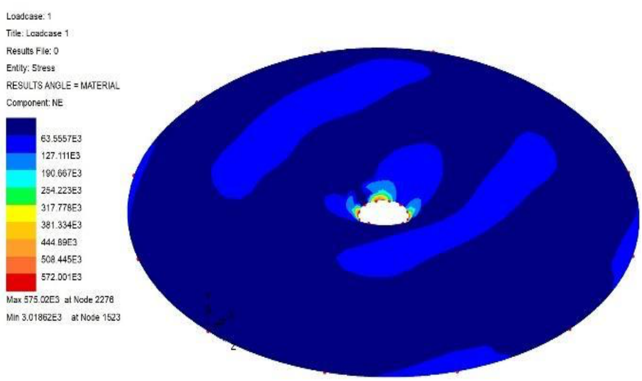 |

Table 5: Stresses contour of cone geometric

<table>
<tr><th>Stresses</th><th>Contour</th></tr>
<tr><td>Stress Resultant in Local X, Nx</td><td>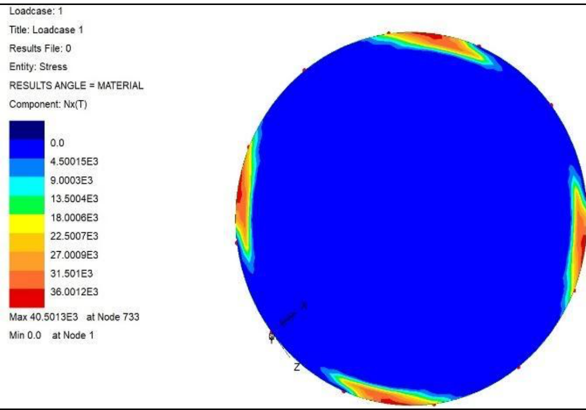
</td></tr>
<tr><td>Stress Resultant in Local Y, Ny</td><td>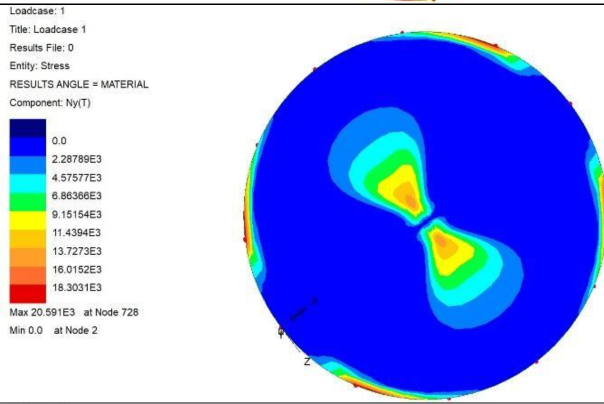
</td></tr>
<tr><td>Equivalent resultant stress, Ne</td><td>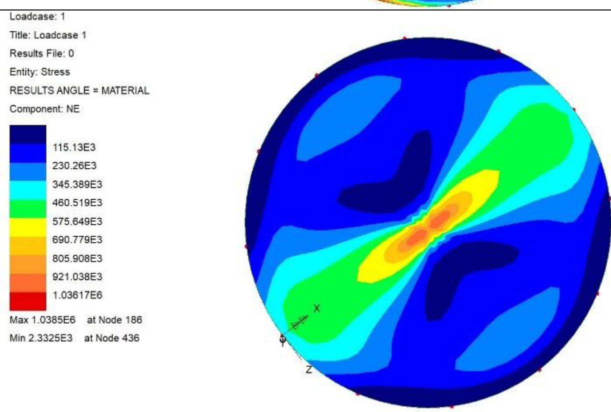
</td></tr>
</table>

Table 6: Stresses of geometric

| Geometric | Equivalent resultant stress, $N_E$ x$10^3$ [N/m] | Maximum stress [N/mm$^2$] |
|---|---|---|
| Dome | 187.3 | 0.62 |
| Toroidal | 575.0 | 1.92 |
| Cone | 1,038.5 | 3.46 |

The cone geometry recorded the highest equivalent resultant stress as the geometry obtained a stress surface profile compared to the dome and toroidal geometries that consisted of a smooth surface profile. Nevertheless, all the geometries proposed recorded lower maximum stress than the strength of the concrete proposed which is 40 N/mm$^2$ [16].

## Artificial Neural Network [ANN]

ANN specializes in recognizing patterns, predicting time series, and modelling [17]. Processing layers are combined using a simple operation that consists of several layers, which are the input, hidden, and output layers [18].

All the proposed geometries were used in the ANN computing system, where all the input data were transposed in Microsoft Excel before being imported into MATLAB. The datasets consisted of the training input, training target, testing input, and testing target. The training input was 70% of the overall data of geometries' node coordinate and node rotation. Meanwhile, the remaining 30% was used as the testing input. The training target used 70% of the deformation data and another 30% was used for the testing target. All the data were extracted from the LUSAS output. A MATLAB tool, nntool, was used to set up the system. The neural network, as shown in Figure 3, was obtained after the nntool manager was completed. After starting the training of the data, regression plots were produced as the output of ANN, as shown in Figure 4. The training parameters differed for each geometry as the value of iterations was varied to achieve the best-fit line in the regression plot.

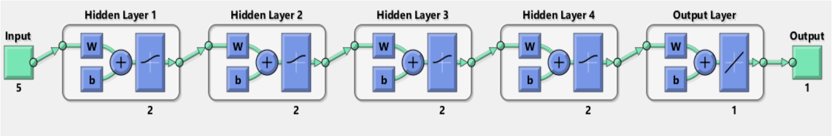


Figure 3: Neural network of ANN.

This study consists of five hidden layers for training, and the testing input comprises five parameters (the node in global direction X, the node in global direction Y, the node in global direction Z, node rotational 1, and node rotational 2). The training and testing output consisted of the sets of node displacement.

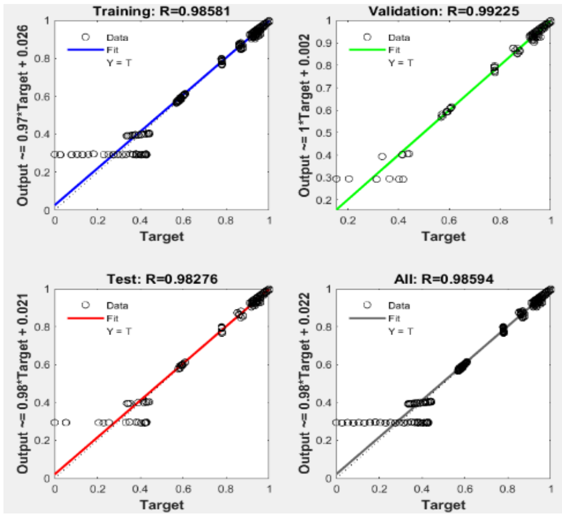


(a)

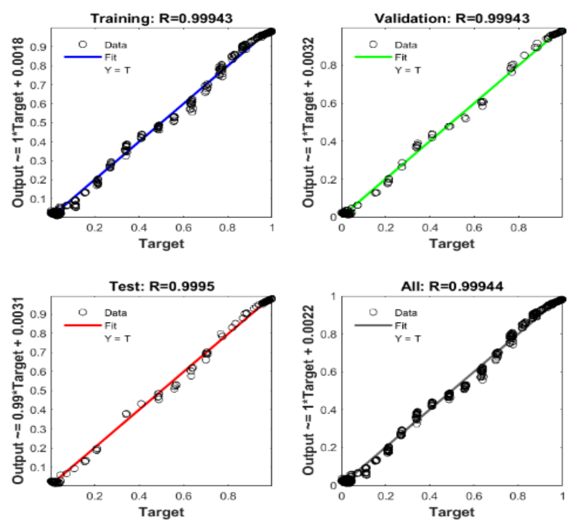


(b)

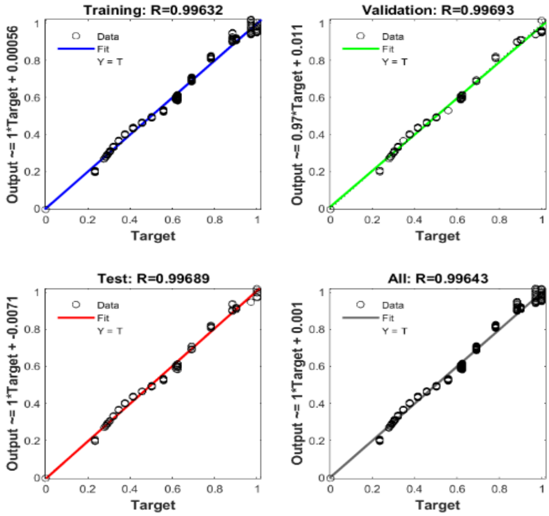


(c)

Figure 4: Regression plots of a) dome geometry, b) toroidal geometry, and c) cone geometry.

Based on the regression plots in Figure 4, all geometries achieved a positive linear function with the correlation coefficient approached the value of 1. This finding indicates that the existing relationship will be stronger as it provides a more linear relationship between the two variables [19]. Based on the ANN computation, the MSE was calculated based on the predicted and actual data, and the results are presented in Table 7. The equation used for MSE calculation is shown in Equation (2) [20]:

$$MSE = \frac{\sum(Actual\ data - Predicted\ data)^2}{\sum Number\ of\ data\ set} \quad (2)$$

Table 7: MSE for ANN data of each geometric

| Geometric | MSE |
|---|---|
| Dome | 0.00000874 |
| Toroidal | 0.00000099 |
| Cone | 0.00000042 |

MSE is commonly used to measure model performance as a standard statistical metric [21]. The error will be lower if the value of MSE is lower. Based on Table 7, the calculated MSE of all proposed geometries approached zero which indicates that the value from actual data extracted from LUSAS is approximately the same as the output from data trained using ANN.

## Conclusion

The proposed elevated shell platform is feasible to be constructed as the foundation platform for township applications because the maximum stresses for all geometries are lower than the design value [22], 40 N/mm$^2$.

MSE was used to define the proposed model from the mathematical equation. The calculated MSE concludes that the three proposed geometries have an almost similar relationship with the models' variables, which are the models' coordinates and rotation as the input and deformation value as the output. The ANN output showed that the predicted data are almost similar to the actual data as all the regression plots approached the value of 1.

Computational analysis of different shell geometries can serve as a useful guideline for structural engineers and aerospace design engineers. Although the structure is used in township applications, some aerospace structures are mainly composed of thin-walled and lightweight structures, such as aircraft and spacecraft [23]. Thus, the design concept of this study can be applied widely for aerospace and conventional constructions because both fields consider the same type of structures.

## References

[1] M. Georgescu, "Long span structures: part 1", *European Erasmus Mundus Master Course*, 2017. https://www.ct.upt.ro/suscos/files/2016-2018/L18_Long%20Span%20Structures.pdf

[2] L. Zhu, N. Li and P. Childs, "Light-weighting in Aerospace Component and System Design", *Propulsion and Power Research*, vol. 7, no. 2, pp. 103-119, 2018.

[3] J. Chilton and C. Chuang, "Rooted in Nature: Aesthetics, Geometry and Structure in the Shells of Heinz Isler", *Nexus Network Journal*, vol. 19, no. 3, pp. 763-785, 2017.

[4] T. Tafsirojjaman, S. Fawzia, D. Thambiratnam and X. Zhao, "Study on the Cyclic Bending Behaviour of CFRP Strengthened Full-scale CHS Members", *Structures*, vol. 28, pp. 741-756, 2020.

[5] A. Hrennikoff, "Discussion of “Analysis of Curved Folded Plate Structures”", *Journal of the Structural Division*, vol. 98, no. 8, pp. 1877-1877, 1972.

[6] R. Rohim, K. Choong. “Structural Behaviour of Origami Inspired Folded Shell Surface.” *World Applied Sciences Journal*, vol. 24, no. 4, pp. 497-502, 2013.

[7] M. Massimo. “Conceptual Design and Analysis of Long Span Structures,” IUAV University of Venice, Italy. 2012.
[8] Public Work Department, "A Guide on Geometric Design of Roads", Arahan Teknik (Jalan) 8/86, 2000.
[9] Department of Irrigation and Drainage, "Floods in Malaysia Historical Reviews, Causes, Effects and Mitigations Approach", 2015.
[10] D. Hegyi, "Numerical Stability Analysis of Arch-supported Membrane Roofs", *Structures*, vol. 29, pp. 785-795, 2021.
[11] R. Taylor, “Interpretation of the Correlation Coefficient: A Basic Review,” *JDMS,* vol. 1, pp. 35-39, 1990.
[12] Veaux, D. R., Velleman, P., & Bock, D., Stats: Data and Models (5th ed.), Boston, Pearson, Addison-Wesley, 2019.
[13] B. J. Goodno and J. M. Gere, *Mechanics of Materials*. Cengage Learning, 2016.
[14] LUSAS©, Version 19, FEA Ltd., 2020.
[15] Kovrizhnykh, A. M., Plane Stress Equations for the Von Mises–Schleicher Yield Criterion, Journal of Applied Mechanics and Technical Physics, vol. 45, no. 6, pp. 894–901 2004.
[16] "BSI Standards, ISO Standards and TSO Publications", *Standardsuk.com*, 2021. [Online]. Available: http://www.standardsuk.com.
[17] A. Shabri, R. Samsudin and Z. Ismail, "Forecasting of the Rice Yields Time Series Forecasting using Artificial Neural Network and Statistical Model", *Journal of Applied Sciences*, vol. 9, no. 23, pp. 4168-4173, 2009.
[18] B. Tarawneh, "Predicting standard penetration test N-value from cone penetration test data using artificial neural networks", *Geoscience Frontiers*, vol. 8, no. 1, pp. 199-204, 2017.
[19] B. Ratner, "The correlation coefficient: Its values range between +1/−1, or do they?", *Journal of Targeting, Measurement and Analysis for Marketing*, vol. 17, no. 2, pp. 139-142, 2009.
[20] S. K. Paul, “Determination of Exponential Smoothing Constant to Minimize Mean Square Error and Mean Absolute Deviation,” *Global Journal of Research in Engineering,* vol. 11, no. 3, 2011.
[21] H. Yee, J. Kim and O. Chong Yong, "Form-Finding Analysis of Tensioned Fabric Structures Using Nonlinear Analysis Method", *Advanced Materials Research*, vol. 243-249, pp. 1429-1434, 2011.
[22] J. He, X. Li, C. Li, J. A. Correia, H. Xin, and M. Zhou, “A novel asynchronous-pouring-construction technology for prestressed concrete box girder bridges with corrugated steel webs,” *Structures*, vol. 27, pp. 1940–1950, 2020.
[23] F. Yuan, “Structural Health Monitoring (SHM) in Aerospace Structures (Woodhead Publishing Series in Composites Science and Engineering) (1st ed.).” *Woodhead Publishing,* pp. 479-495, 2016.